# Cell-size distribution and scaling in a one-dimensional Kolmogorov-Johnson-Mehl-Avrami lattice model with continuous nucleation

Zoltán Néda,* Ferenc Járai-Szabó, and Szilárd Boda
*Babeş-Bolyai University, Department of Physics, RO-400084, Cluj-Napoca, Romania*
(Received 9 June 2017; revised manuscript received 19 August 2017; published 20 October 2017)

The Kolmogorov-Johnson-Mehl-Avrami (KJMA) growth model is considered on a one-dimensional (1D) lattice. Cells can grow with constant speed and continuously nucleate on the empty sites. We offer an alternative mean-field-like approach for describing theoretically the dynamics and derive an analytical cell-size distribution function. Our method reproduces the same scaling laws as the KJMA theory and has the advantage that it leads to a simple closed form for the cell-size distribution function. It is shown that a Weibull distribution is appropriate for describing the final cell-size distribution. The results are discussed in comparison with Monte Carlo simulation data.

DOI: 10.1103/PhysRevE.96.042145

## I. INTRODUCTION

The Kolmogorov-Johnson-Mehl-Avrami (KJMA) growth model [1–3] has large applicability for describing several natural phenomena [4–6] such as domain growth associated with isothermal phase transformation [7–10], random sequential adsorption processes [5,11], and thin-film growth [12]. Recently, the model found exotic applications in molecular biology [13] and cosmology [14], as well. The Voronoi-type space tessellations [15] that appear as the result of growth have also diverse scientific applications in physics, biology, materials science, computer science, astrophysics, medicine, economics, and sociology (see for example [15–17] and the references within these works).

Although the KJMA model has been extensively studied (see for example [18–23]) and in one-dimension (1D) exact results are known for the cell-size distribution function [18,23,24], the nonanalytical form of the results limits their applicability. We propose here an alternative, approximative theory, different from the one known to the KJMA process. Due to the involved approximations our results are not exact and less accurate than the one given by the the KJMA theory in 1D. However, the advantage of our approach is that it leads to the same scaling laws as the exact theory in 1D and suggests a simple analytical form for the cell-size distribution function. The situation is somewhat similar to the case of the Poissonian Voronoi cell-size distribution function, where a simple and reasonably fair fit with a few parameters proves to be more useful for practical applications than a complicated albeit more exact form [16].

In the following first we present our lattice model and adapt its results for the 1D KJMA process. Then, we present our simple mean-field-like analytical approximation for the studied quantities. Finally we present Monte-Carlo-type computer simulation data for this growth process and compare critically the obtained results with the theoretical ones.

## II. THE LATTICE MODEL

The model considered here is the lattice version of the KJMA model with continuous nucleation in 1D. The term "continuous nucleation" as it is used in the literature (see for example [24]) refers to the fact that new cells can continuously nucleate on empty sites with a constant rate. We consider discrete time steps, and therefore fix a constant probability, to nucleate a new cell on an empty site in each simulation step. The growth process is sketched in Fig. 1. At the $t = 0$ time step all sites are empty. At any $t > 0$ time step, each empty site can be activated with a probability $p$, leading to a new cell (depicted in the figure with different colors). The existing cells can grow then (in the same time step) at both of their end points by occupying the neighboring empty cells. Whenever two cells get in contact, the growth stops at that boundary. The growth order for the cells is fully randomized. In such manner if there is only one empty site between two neighboring cells, this site will be occupied with the same $1/2$ probability by one of the two involved cells. The nucleation and growth dynamics continue until all sites are occupied by these Voronoi-like cells. The model as described above has two parameters: the size of the one-dimensional lattice, $L$, and the nucleation probability, $p$.

Another variant of the model would be when in each time step first the growth process is considered and after that nucleation of new cells on the remaining empty sites. By performing a Monte Carlo simulation exercise it is easy to show that for large lattices and small enough $p$ values the two different updates lead to statistically similar final configurations and scaling relations.

We are investigating the time $t_{\mathrm{sat}}$, needed to get saturation and the statistics of the Voronoi-like cells at the end of the growth process. More specifically, we would like to determine the mean cell size $c$ and the probability distribution function for the cell sizes. Our aim is to get a compact analytical approximation for the distribution function, one that would be useful in practical applications.

Due to the discrete nature of time and space one has to be very careful in generalizing the results of the KJMA theory for describing the results of this model. The KJMA theory considers continuous space and time, and the discrete lattice model should reproduce this limit only for infinitely large lattices and very small nucleation probabilities. A major conceptual difference is that in the continuous KJMA model the $t_{\mathrm{sat}}$ saturation time is infinite, and if one wants to define such a quantity to compare model results with some experiments,

*zneda@phys.ubbcluj.ro

 

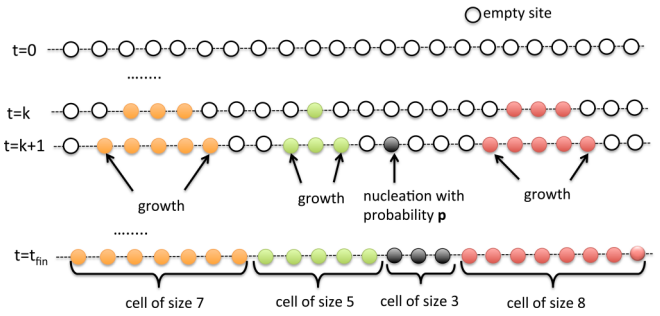


FIG. 1. Sketch of the 1D KJMA lattice model dynamics.

it usually defines the saturation time as the time needed to transform a fixed percentage of volume (for example 99%) in the new phase. Finite-size effects that are present in the lattice model are also not applicable for the KJMA model.

## III. THE CLASSICAL KJMA THEORY IN 1D

The KJMA model corresponding to our growth model is the one which is known in the literature as the *continuous nucleation model* [1–3], where each cell (grain) is physically distinguishable from the others (or represent a different phase). The model is defined in continuous space and time. In our discrete growth mechanism we define the length unit $l$ as the distance between two neighboring lattice sites, and the unit time $T$ is set to one growth step, as described earlier. The original model in its general form is governed by two parameters, $p$ the new cell nucleation rate per unit length and $v$, the linear velocity at which the cells grow in both directions until impeded by a neighboring cell. In our lattice approach an additional parameter is the size $L$ of the 1D lattice. The growth described in the previous section sets the time unit by considering $v = 1\,l/T$.

Following the seminal work of Axe and Yamada [18] it is easy to realize that the model has a dimensional scaling. Using the nucleation rate $p$ (dimension $l^{-1}T^{-1}$) and the growth velocity $v$ (dimension $lT^{-1}$) we can define a natural length and time scale for the KJMA growth process in 1D as

$$\xi = (p/v)^{-1/2}, \tag{1}$$

$$\theta = (pv)^{-1/2}. \tag{2}$$

This allows for any $G(s,t)$ function that is related to the space-time evolution of the system ($s$ is the spacial coordinate and $t$ the timelike coordinate) to be rescaled in a universal form by expressing $s$ and $t$ in the $\xi$ and $\theta$ units. This observation immediately implies that for the case in which we use instead of $s$ the rescaled length $x = s/\xi$ and instead $t$ the rescaled time $\tau = t/\theta$ there is a universal cell-size distribution function independent of $p$ and $v$.

It is worth mentioning here also that in our lattice model (see Sec. II) we have fixed $v = 1$. The results obtained for this specific case can be however easily generalized for arbitrary $v$ values by using a dimensional analysis and the natural length and time scales from (2).

In the continuous growth model Kolmogorov [1] derived the famous result

$$w(t) = \frac{W(t)}{L} = \exp[-V_{ex}(t)] \tag{3}$$

for the fraction of untransformed material at time $t$. In the above equation $W(t)$ denotes the amount of material occupied by the growing cells, $L$ is the total size of the space where the growth takes place, and $V_{ex}(t)$ denotes the *total extended volume fraction*. The total extended volume is defined as the hypothetical volume of the cells at time moment $t$ if their growth were unimpeded by the other cells (i.e., in the absence of collision with other cells), divided by the size of the space where the growth takes place. The value of $V_{ex}(t)$ in 1D is

$$V_{ex}(t) = \frac{1}{L}\int_0^t pL\,2vt'\,dt' = pvt^2, \tag{4}$$

and we get

$$w(t) = \exp(-pvt^2). \tag{5}$$

Following the works of Kolmogorov [1] and Avrami [3] we can also estimate the number of nucleated cells $N(t)$ at time moment $t$ as

$$N(t) = Lp\int_0^t w(t')dt' = L\sqrt{\frac{p}{v}}\int_0^{t\sqrt{pv}} \exp(-u^2)du. \tag{6}$$

For arbitrary $t$ time this leads to a nonanalytical form, which can be expressed by using the *error function*. In the limit of $t \to \infty$ we get the total number of cells as

$$N_t = N(\infty) = L\frac{\sqrt{\pi}}{2}\sqrt{\frac{p}{v}}, \tag{7}$$

which leads us to the average cell size $c$ in the final configuration:

$$c = \frac{L}{N_t} = \frac{2}{\sqrt{\pi}}\sqrt{\frac{v}{p}}. \tag{8}$$

For our finite 1D lattice with size $L$ we can estimate also the time needed to get saturation. The time needed to get $w(t) = 0$ is infinitely long. Usually the saturation time is estimated by imposing a given percentage of the transformation reached, for example $\kappa = 0.99$. In such case the saturation time can be estimated by imposing

$$w\left(t_{\text{sat}}^{\text{cont}}\right) = 1 - \kappa, \tag{9}$$

which leads to an approximation for the saturation time in the continuous KJMA model:

$$t_{\text{sat}}^{\text{cont}} = \frac{1}{\sqrt{pv}}\sqrt{-\frac{1}{\ln(1-\kappa)}} \propto \frac{1}{\sqrt{pv}}. \tag{10}$$

This result is obviously independent of the system size and therefore there are no finite-size effects.

However, on our finite lattice there is a a finite saturation time. The condition for saturation is to get the total number of nonoccupied sites less than one. This leads to the saturation condition

$$W(t_{\text{sat}}) = 1. \tag{11}$$

The estimate for the $t_{sat}$ time length of the growth is

$$t_{sat} = \sqrt{\frac{\ln L}{pv}}. \tag{12}$$

In the definition of our discrete lattice model we considered $v = 1$. In such case according to the KJMA theory we would expect the following scaling properties:

$$c = \frac{2}{\sqrt{\pi}}\frac{1}{\sqrt{p}} \propto \frac{1}{\sqrt{p}}, \tag{13}$$

$$t_{sat} = \sqrt{\frac{\ln L}{p}} \propto \frac{1}{\sqrt{p}}. \tag{14}$$

An exact theoretical method for getting the grain-size distribution in the 1D KJMA models has been known for a quite long time; see for example the works of Axe and Yamada [18], Ben-Naim and Krapivsky [24], or Farjas and Roura [23]. The problem with these approaches is that they do not lead to a compact analytic form, only to a numerically computable density function, which is not practical for fitting experimental data. We consider thus an alternative, less accurate theory for the 1D KJMA growth, which yields an analytically compact form for the density function of the cell-size distribution.

## IV. MEAN-FIELD-LIKE APPROACH

Let us consider the 1D growth in a mean-field (MF) type approach. "Mean field" means here that we assume no correlation effects between the growing cells, and we treat the distribution of empty sites as a completely random distribution.

We denote by $p$ the site activation probability and by $L$ the total number of lattice sites. At each time moment $t$ let $N(t)$ be the total number of cells and $W(t)$ the number of empty (nonactivated) lattice sites. The probability that a randomly chosen site is empty at time moment $t$ is

$$q(t) = \frac{W(t)}{L}. \tag{15}$$

The dynamics of the $N(t)$ and $W(t)$ quantities are described by the following equations:

$$\frac{dN(t)}{dt} = pW(t), \tag{16}$$

$$\frac{dW}{dt} = -2q(t)N(t) - pW(t). \tag{17}$$

The term $2q$ results in the following manner. The probability that a cell grows on both of its sides [leading to a 2-site decrease in $W(t)$] in a unit time step is $q^2$. The probability that a cell grows only in one given direction is $q(1-q)$. In such case the newly occupied site can be the left or the right one, both of them leading in $W(t)$ to a decrease with 1 site. Therefore the number of sites that are getting occupied by the growth of the cell is $[2q^2 + 2q(1-q)]N(t) = 2qN(t)$. The second term in Eq. (17) results from the fact that each empty site can be activated with a probability $p$.

In such manner we get a solvable system of coupled first-order differential equations for $N(t)$ and $W(t)$. Using Eq. (15) we get

$$\frac{dN(t)}{dt} = pW(t), \tag{18}$$

$$\frac{dW}{dt} = -2\frac{W(t)}{L}N(t) - pW(t), \tag{19}$$

which should be solved with the initial conditions

$$N(0) = 0, \tag{20}$$

$$W(0) = L. \tag{21}$$

The solution of the system is

$$N(t) = -\tfrac{1}{2}pL + \tfrac{1}{2}L\sqrt{p(p+4)}F(t), \tag{22}$$

$$W(t) = L\left[1 + \frac{p}{4} - F(t)^2 - \frac{p}{4}F(t)^2\right], \tag{23}$$

where

$$F(t) = \tanh\left[\frac{1}{2}\left(\sqrt{p(4+p)}t + 2\tanh^{-1}\sqrt{\frac{p}{4+p}}\right)\right]. \tag{24}$$

In the limit of $p \ll 1$, which is our case, we can keep only the leading terms in $p$ and we get the simplified solution of the system

$$N(t) \approx L\sqrt{p}F(t), \tag{25}$$

$$W(t) \approx L[1 - F(t)^2], \tag{26}$$

where

$$F(t) \approx \tanh\left[\sqrt{p}\left(t + \tfrac{1}{2}\right)\right]. \tag{27}$$

Since one time unit is equivalent to one step in the growth process, apart from the very beginning of the dynamics we can assume $(t+1) \approx t$, leading to

$$F(t) \approx \tanh\left(\sqrt{p}t\right). \tag{28}$$

According to these results, the *total number of cells*, $N_t$, at the end of the growth process can be approximated as

$$N_t = \lim_{t\to\infty} N(t) \approx L\sqrt{p}. \tag{29}$$

The *mean cell size* $c$ will be given by

$$c = \lim_{t\to\infty} \frac{L}{N(t)} \approx \frac{1}{\sqrt{p}}. \tag{30}$$

The scaling property as a function of $p$ is the same as the result of Eq. (13) given by the KJMA theory. The saturation time necessary to fill up all sites $t_{sat}$ will be estimated now in the same manner as in the classical KJMA theory,

$$W(t_{sat}) = 1, \tag{31}$$

and consequently

$$F(t_{sat}) = \sqrt{1 - \frac{1}{L}}. \tag{32}$$

From here one gets

$$t_{sat} = \frac{1}{\sqrt{p}}\tanh^{-1}\sqrt{1 - \frac{1}{L}}. \tag{33}$$

Taking into account that $1/L = \epsilon \ll 1$, we can perform a Taylor expansion of the $\tanh^{-1}(\sqrt{1-\epsilon})$ term around $\epsilon = 0$, and we get

$$\tanh^{-1}(\sqrt{1-\epsilon}) \approx \ln(2) - \tfrac{1}{2}\ln(\epsilon) - \tfrac{1}{8}\epsilon + O(x)^2. \quad (34)$$

This leads us to

$$t_{\rm sat} \approx \frac{1}{2\sqrt{p}}\ln(4L), \quad (35)$$

suggesting for constant $L$ the same scaling as the KJMA theory in 1D [Eq. (14)],

$$t_{\rm sat} \propto \frac{1}{\sqrt{p}}. \quad (36)$$

The finite-size effect, i.e., variation of $t_{\rm sat}$ as a function of $L$, is however different.

We proceed now to determine the *size-distribution function* of the cells in the limit where we neglect $q(t)^2$ and keep only the leading terms in $p$, i.e., where the solutions given by Eqs. (25), (26), and (27) are valid. If we denote the number of cells of size $k$ at time moment $t$ by $N(k,t)$, the dynamics of the system can be written by a coupled system of master equations. For cells of sizes 1 and 2, the equations are a little different, but for $k > 2$ the growth equations have the same form:

$$\begin{aligned}
&\frac{dN(1,t)}{dt} = pLq - N(1,t)(2q-q^2),\\
&\frac{dN(2,t)}{dt} = N(1,t)2q(1-q) - N(2,t)(2q-q^2),\\
&\cdots,\\
&\frac{dN(k,t)}{dt} = N(k-2,t)q^2 + N(k-1,t)2q(1-q)\\
&\qquad\qquad - N(k,t)(2q-q^2),\\
&\cdots.
\end{aligned} \quad (37)$$

Keeping only the first-order terms in $q$,

$$\begin{aligned}
&\frac{dN(1,t)}{dt} = pLq - 2qN(1,t),\\
&\cdots,\\
&\frac{dN(k,t)}{dt} = 2qN(k-1,t) - 2qN(k,t),\\
&\cdots,
\end{aligned} \quad (38)$$

we introduce the

$$P_i(k,t) = \frac{N_i(k,t)}{N(t)} \quad (39)$$

probabilities of finding a cell with size $k$ among all cells in the system at time moment $t$. Its first-order time derivative is

$$\frac{dP_i(k,t)}{dt} = \frac{1}{N(t)}\frac{dN(k,t)}{dt} - \frac{1}{N(t)^2}\frac{dN(t)}{dt}N(k,t). \quad (40)$$

Using Eqs. (15) and (16) we can write

$$\frac{dP_i(k,t)}{dt} = \frac{1}{N(t)}\frac{dN(k,t)}{dt} - pq(t)P(k,t)\frac{L}{N(t)}. \quad (41)$$

We rewrite now the master equations (38) for the corresponding probabilities:

$$\begin{aligned}
&\frac{dP(1,t)}{dt} = \frac{L}{N(t)}pq - 2qP(1,t) - pqP(1,t)\frac{L}{N(t)},\\
&\cdots,\\
&\frac{dP(k,t)}{dt} = 2qP(k-1,t)q - 2qP(k,t) - pqP(k,t)\frac{L}{N(t)},\\
&\cdots.
\end{aligned} \quad (42)$$

The master equation for the cumulative distribution function

$$S(k,t) = \sum_{i=1}^{k} P(k,t) \quad (43)$$

can be obtained by adding up the equations in (42):

$$\frac{\partial S(k,t)}{\partial t} = -[S(k,t) - S(k-1,t)]2q + \frac{pqL}{N(t)}[1 - S(k,t)]. \quad (44)$$

Let us consider now the continuous limit of this probability distribution, and instead of $P(k,t)$ let us use the probability density $\Omega(s,t)$, where $s$ is a continuous variable. Equation (44) becomes now a partial differential equation (PDE) of the form

$$\frac{\partial\Omega(s,t)}{\partial t} = -2q\frac{\partial\Omega(s,t)}{\partial s} + \frac{pqL}{N(t)}[1-\Omega(s,t)]. \quad (45)$$

Using the result from Eq. (25) for $N(t)$ and Eq. (26) for $W(t)$, we get the following PDE for the distribution function:

$$\frac{\partial\Omega(s,t)}{\partial t}\frac{F(t)}{1-F(t)^2} + 2F(t)\frac{\partial\Omega(s,t)}{\partial s} = \sqrt{p}[1-\Omega(s,t)]. \quad (46)$$

For $F(t)$ given by Eq. (28) one obtains

$$\begin{aligned}
&\frac{\partial\Omega(s,t)}{\partial t}\frac{\tanh(t\sqrt{p})}{1-\tanh^2(t\sqrt{p})} + \frac{\partial\Omega(s,t)}{\partial s}\tanh(t\sqrt{p})\\
&\quad = \sqrt{p}[1-\Omega(s,t)].
\end{aligned} \quad (47)$$

This is an equation that is independent of $L$. We can also show that the evolution equation for the cumulative distribution function will be independent of the parameter $p$ if we use the cell size relative to the mean cell size and rescale the time properly. More precisely, let us consider the following scalings: $x = s/c = s\sqrt{p}$ (where $c$ denotes the average cell size) and $\tau = t\sqrt{p}$. With these new variables we get

$$\frac{\partial\Omega(x,\tau)}{\partial\tau}\frac{\tanh(\tau)}{1-\tanh^2(\tau)} + 2\frac{\partial\Omega(x,\tau)}{\partial x}\tanh(\tau) = [1-\Omega(x,\tau)], \quad (48)$$

which is obviously independent of $p$, suggesting a scaling property for the cell-size distribution function. This result confirms again the consequences of the scaling relations given by Eq. (2).

The general solution of this first-order partial differential equation obtained with the standard mathematical methods is

written as

$$\Omega(x,\tau) = 1 - \frac{1}{\tanh(\tau)} e^{H[x-2\tanh(\tau)]}, \tag{49}$$

with $H[z]$ an arbitrary function. Since $\Omega(x,\tau)$ is the cumulative cell-size distribution function, we search for a general solution satisfying the criteria $\Omega(\infty,\tau) = 1$, $\Omega(0,\infty) = 0$, and $d\Omega(x,\tau)/dx > 0$ for all $x$ values. Taking into account that $0 \leqslant \tanh(x) \leqslant 1$, a general class of function $H[z]$ satisfying the imposed conditions is $H[z] = -\gamma(z+2)^{\alpha}$, where $\gamma$ and $\alpha$ are two positive constants. This leads to the cumulative cell-size distribution function

$$\Omega(x,\tau) = 1 - \frac{1}{\tanh(\tau)} e^{-\gamma[x-2\tanh(\tau)+2]^{\alpha}}. \tag{50}$$

It is easy to verify that such a solution satisfies the partial differential equation (48). The above solution leads for $\tau \to \infty$ to the final cumulative cell-size distribution function:

$$\Omega(x) = 1 - e^{-\gamma x^{\alpha}}. \tag{51}$$

The corresponding probability density function is

$$\rho(x) = \gamma\alpha x^{\alpha-1} e^{-\gamma x^{\alpha}}, \tag{52}$$

which is the well-known Weibull distribution. Taking into account that $\langle x \rangle = 1$, we get

$$\gamma = \left[\Gamma\left(1 + \frac{1}{\alpha}\right)\right]^{\alpha}, \tag{53}$$

with $\Gamma(x)$ the classical Gamma function.

## V. COMPUTER SIMULATIONS

In order to check the theoretical predictions Monte-Carlo-type computer simulations have been performed. We have considered system sizes up to $L_{\max} = 10^9$ lattice sites and varied the nucleation probability in the range of $10^{-2} \leqslant p \leqslant 10^{-7}$. Simulations were done by performing in each time step the growth of the existing cells first, and after that considering the nucleation possibilities of new cells. It has been verified however that the results are unchanged for the case in which the order of the two process is inverted.

First, we have studied the statistical properties for the time evolution of the system. Considering lattices with $L = 10^8$ sites and various nucleation probability values, we followed the fraction of transformed phase $w(t) = W(t)/L$ as a function of time. Simulation results averaged on $Q = 100$ realizations are plotted with continuous lines in Fig. 2. The prediction of the KJMA theory (blue squares) describes well the simulation results. As expected, our MF theory (dashed red line) gives a fair description at the beginning of the dynamics, where the cell's growth can be considered independent, and a considerable deviation is observed for later time steps.

The $t_{\text{sat}}$ time length of the growth process until saturation will be our focus now. The results are presented in Figs. 3 and 4. In Fig. 3 symbols represents the computer simulation results obtained for the scaling of the saturation time as a function of the nucleation probability. Results for systems with different sizes $L$ are presented as indicated in the legend. The results are averaged on many configurations, indicated by the $Q$ values in the legend. Black lines indicate the prediction obtained from the KJMA theory [Eq. (14)] and red lines indicate our MF prediction given by Eq. (35). The observed trend suggest that the scaling predicted by both theories, $t_{\text{sat}} \propto p^{-1/2}$, is correct. The actual values for $t_{\text{sat}}$ given by the KJMA theory are however much better in this case than the results of the MF theory.

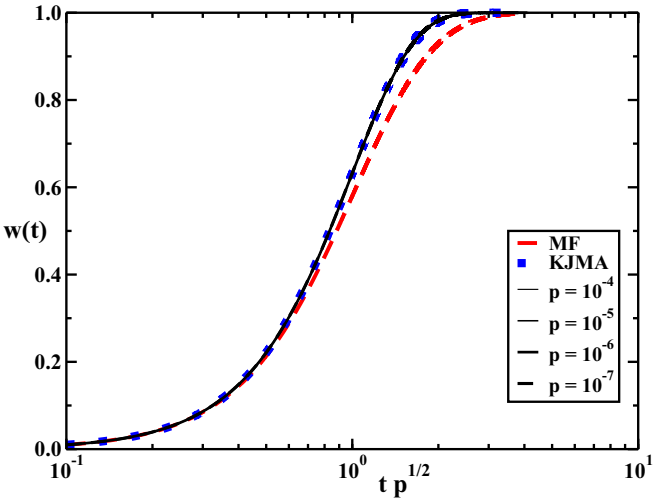


FIG. 2. Fraction of activated sites (transformed phase), $w = W(t)/L$, as a function of time. Continuous curves are computer simulation results obtained for lattices with $L = 10^8$ sites and for various nucleation probabilities $p$, averaged on $Q = 100$ realizations. Blue squares are the prediction of the KJMA theory, while the red dashed line is the result given by the MF theory.

From the theoretical predictions we expect that the saturation time is a function of the system size $L$. The computer simulation results plotted in Fig. 3 confirm this expectation. This finite-size effect is studied for different nucleation

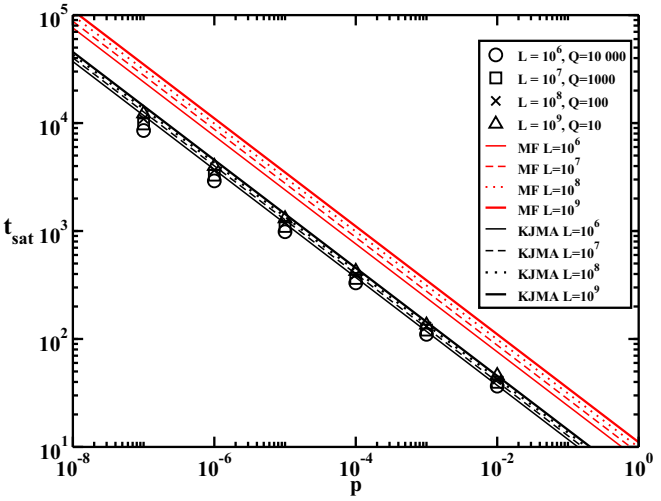


FIG. 3. Time needed for saturation, $t_{\text{sat}}$, as a function of the nucleation probability, $p$. Computer simulation results (circles) are obtained on lattice sizes $L$ and averaged on $Q$ realizations as indicated in the legend. Black lines represent the prediction of the KJMA theory given by Eq. (14). Red lines indicate our MF prediction given in Eq. (35).

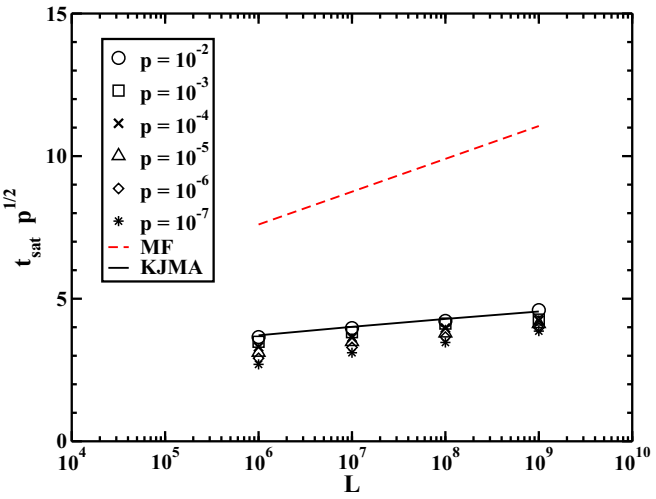


FIG. 4. Saturation time, $t_{\rm sat}$, as a function of the system size. Simulation results (symbols) are for different $p$ values indicated in the legend. The data is averaged on many configurations $Q$ which is changing with the system size $L$ (the same $Q$ values are used as in case of Fig. 3). The dashed line indicates the upper bond given by Eq. (35).

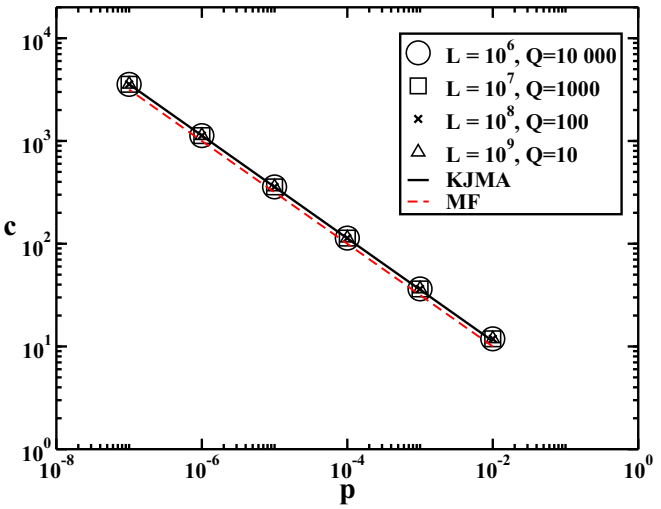


FIG. 5. Mean cell size as a function of the $p$ nucleation probability. Computer simulations were realized on lattices with different sizes $L$ and averaged on $Q$ realizations as it is indicated in the legend. The continuous black line represents the prediction of the KJMA theory [Eq. (13)] and the red dashed line is our MF prediction given in Eq. (30).

probabilities and the results are plotted in Fig. 4. In order to collapse the data for different $p$ values we have plotted $t_{\rm sat}\,p^{1/2}$ as a function of the system size. Symbols represent computer simulation data for different $p$ values. The data are averaged on many configurations $Q$ that are changing with the system size $L$. Here, the same $Q$ values are used as in the case of Fig. 3. The continuous black line indicates the KJMA prediction, Eq. (14), while the red dashed line is the result in Eq. (35), obtained by the MF theory. The result obtained from the KJMA theory gives a good approximation for the computer simulation data. The increasing trend of the MF theory is correct; however the actual results offer a much weaker approximation than the ones of the KJMA theory. One should also note that the result of the KJMA theory adapted to the lattice model, Eq. (14), is also not perfect. The data for different $p$ values suggests that even the $t_{\rm sat} \propto p^{-1/2}$ scaling hypothesis is not rigorously exact for describing our MC simulations on the lattice. This is suggested by the slightly different slopes observed for the simulation results of $t_{\rm sat}$ as a function of $p$, plotted on log-log scales for different system sizes, $L$ (different symbols in Fig. 3). Again, we emphasize that this difference does not mean that the KJMA theory is not exact; it just shows that applying the results of the continuous KJMA theory to the MC simulation results obtained on finite lattices has to be done with much care and finite-size effects have to be taken into account.

We discuss now the statistical results for the final cell-size distribution. Results for the mean cell size, $c$, as a function of the nucleation probability are given in Fig. 5. Here, the symbols represent simulation results for different system sizes, $L$, and averaged on $Q$ realizations (as indicated in the legend). The continuous black line indicates the result of the KJMA theory given by Eq. (13) and with the red dashed line we plot our MF prediction given in Eq. (30). The computer experiments confirm nicely the $c \propto p^{-1/2}$ scaling. Although the KJMA theory offers a perfect description for the results, the values predicted in the MF approach gives also a surprisingly good approximation.

The final cell-size distribution function was studied for different system sizes and nucleation probabilities. For the $\rho(x)$ probability density functions, where the cell size is normalized by the mean cell size ($x = s/c$), the collapse of the distribution functions for different $p$ and $L = 10^8$ sites is shown in Fig. 6. Here, the distribution function is obtained from $Q = 100$ different simulations resulting in $N_{\rm cells}$ individual

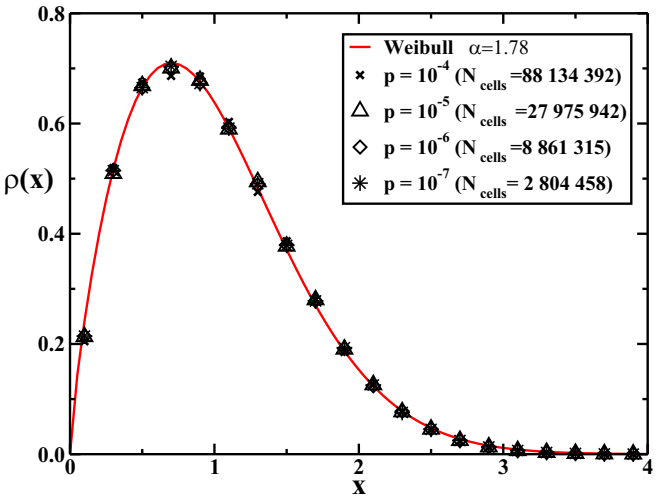


FIG. 6. Final cell-size distributions, $\rho(x)$, obtained for different $p$ nucleation probabilities (as indicated in the legend) and $L = 10^8$ system size. The continuous curve shows a Weibull fit with $\alpha = 1.78$ for the collapsed data. Simulation results are generated from $Q = 100$ different runs, which result in $N_{\rm cells}$ individual cells (indicated in the legend).

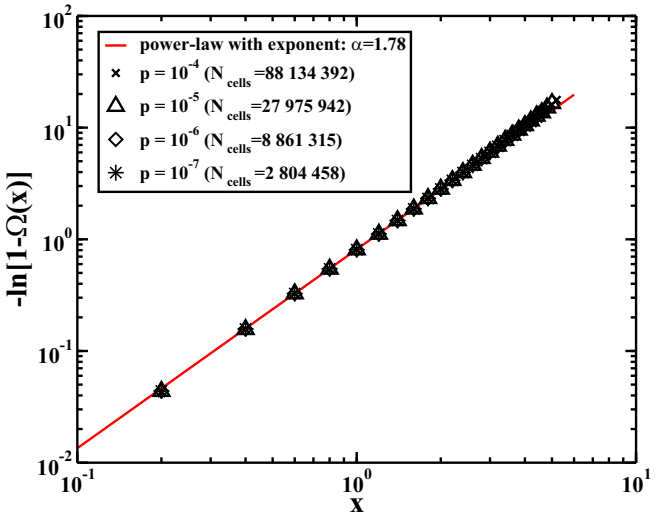


FIG. 7. Scaling properties related to the final cumulative cell-size distribution. The linear trend on the log-log plot for $-\ln[1-\Omega(x)]$ suggests that the Weibull distribution function with $\alpha = 1.78$ describes well the computer simulation data. Symbols indicate computer simulation results for different nucleation probabilities, as specified in the legend. The continuous red line is a power law with exponent 1.78. Simulation results were obtained on lattices with $L = 10^8$ sites and calculated from $Q = 100$ different runs which result in $N_{\text{cells}}$ individual cells (indicated in the legend).

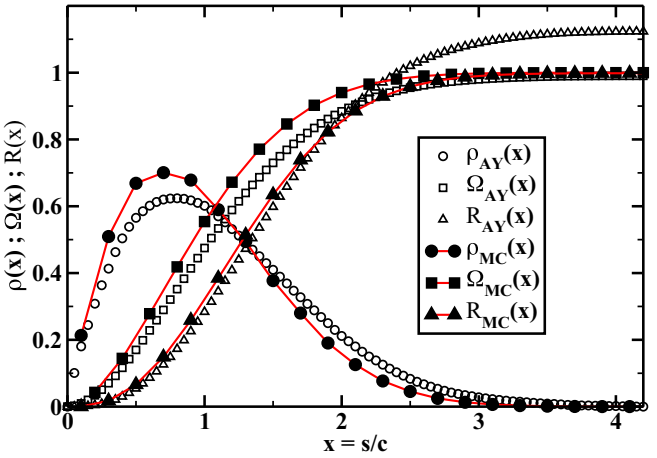


FIG. 8. Results in comparison with the ones numerically computed and plotted by Axe and Yamada [18]. Black dots are our simulation results for the $\rho(x)$ density function, and the circles are the corresponding numerical results of Axe and Yamada. Filled black squares are MC simulation results for the cumulative cell-size distribution function, $\Omega(x)$, and the empty squares are the results calculated form the work of Axe and Yamada. Filled triangles are the $R(x)$ values computed for our simulation results from Eq. (54) and the empty triangles are the $R(x)$ values calculated from the numerical results of Axe and Yamada.

cells indicated in the legend. In the same figure we also indicate that a Weibull fit [see Eq. (52)] with $\alpha = 1.78$ works well.

To further argue the Weibull form of the final cell-size distribution function, we have plotted $-\ln[1-\Omega(x)]$ as a function of $x$ in Fig. 7 [we recall that $\Omega(x)$ is the cumulative distribution function]. If one accepts for $\Omega(x)$ the Weibull distribution given by Eq. (51), than a power-law trend is expected for $-\ln[1-\Omega(x)]$. The straight trend of the simulation results in a log-log plot indicates a fair scaling with an exponent of $\alpha = 1.78$. This gives us further evidence that the Weibull distribution is appropriate for describing the final cell-size distribution for the 1D KJMA lattice model with continuous nucleation.

## VI. DISCUSSION AND CONCLUSIONS

We have considered a KJMA growth process with continuous nucleation on one-dimensional lattices. In order to investigate the growth dynamics, the total time of the growth process, and the statistics of the final cell-size distribution, we used both the classical KJMA theory and a mean-field (MF) type approximation. Computer simulation results were compared with the predictions of these theories. We found that the KJMA theory can be adapted to this discrete model and offers an excellent description for the statistical properties of the growth process. The lack of a compact form for the cell-size distribution function is however a great impediment. The MF-type approximation gives a good description for the initial part of the dynamics, where the growth of the cells can be considered as independent and coalescence is not important. The MF theory leads to the same scaling properties for the saturation time and mean cell size as a function of the nucleation probability as the KJMA theory. However, the advantage of the MF-type approach is that it leads to a compact analytical approximation for the final cell-size distribution function. According to this, we expect a Weibull distribution. The importance of such a compact formula can be immediately exemplified by discussing the $\rho(x)$ distribution function plotted in Fig. 2 in the seminal work of Axe and Yamada [18]. In this figure, the authors numerically compute and plot the $\rho(x)$ normalized distribution function ($x = s/c$ with $c$ the mean cell size). This plot should be thus identical with the one given in our Fig. 6. In Fig. 8 we have replotted the digitized results of Axe and Yamada together with our MC simulation data which are almost perfectly fitted by the one-parameter Weibull distribution. One can immediately observe however that the two curves do not mach. Although both of the density functions are properly normalized (see the trend in the cumulative distribution function, plotted in Fig. 8) one of them should be wrong. We can immediately recognize that there is a mistake in the density function plotted in Ref. [18], by computing the

$$R(x) = \int_0^x \rho(y)\, y\, dy \tag{54}$$

integral. According to the definition of $x$ one should have $\lim_{x\to\infty} R(x) = 1$. In Fig. 8 we observe that while the MC simulation results indicate the right trend for $R(x)$, the curve plotted by Axe and Yamada fails. This is a clear sign that due to the extremely complicated manner in which the $\rho(x)$ density function was numerically computed in Ref. [18], mistakes were made. The compact form for the $\rho(x)$ distribution function offered by our mean-field-type approximation is

appropriate to avoid such mistakes and therefore is more appropriate for any practical applications in fitting experimental data.

Unfortunately, it is not obvious how one could extend the MF-type approach for computing the final cell-size distribution function in higher-dimensional KJMA models with continuous nucleation. We have also checked by MC simulations that a Weibull distribution is not appropriate for the density function of the 2D and 3D KJMA models. One can easily make the extension of the MF theory for predicting the scaling properties for the mean cell size and saturation times in 2D and 3D, but as we have seen already here, the KJMA theory offers already exact and compact results for these problems. In such sense the problem of giving a compact analytical approximation for the cell-size distribution function of the KJMA growth model with continuous nucleation remains an open problem for the practically important 2D and 3D cases.

## ACKNOWLEDGMENT

This work is supported by Romanian UEFISCDI Grant No. PN-III-P4-PCE-2016-0363.

[1] A. N. Kolmogorov, Bull. Acad. Sci. URSS (Cl. Sci. Math. Nat.) **3**, 355 (1937).
[2] W. A. Johnson and R. F. Mehl, Trans. Am. Inst. Min. Metall. Pet. Eng. **135**, 416 (1939).
[3] M. Avrami, J. Chem. Phys. **7**, 1103 (1939); **8**, 212 (1940).
[4] M. Fanfoni and M. Tomellini, Nuovo Cimento D **20**, 1171 (1998).
[5] J. W. Evans, Rev. Mod. Phys. **65**, 1281 (1993).
[6] R. A. Ramos, P. A. Rikvold, and M. A. Novotny, Phys. Rev. B **59**, 9053 (1999).
[7] J. W. Christian, *The Theory of Phase Transformations in Metals and Alloys, Part I: Equilibrium and General Kinetic Theory* (Pergamon Press, New York, 1981).
[8] Y. Ishibashi and Y. Takagi, J. Phys. Soc. Jpn. **31**, 506 (1971).
[9] D. W. Henderson, J. Non-Cryst. Solids **30**, 301 (1979).
[10] A. A. Hirsch and G. Galeczki, J. Magn. Magn. Mater. **114**, 179 (1992).
[11] J. Feder, J. Theor. Biol. **87**, 237 (1980).
[12] B. Lewis and J. C. Anderson, *Nucleation and Growth of Thin Films* (Academic Press, New York, 1978).
[13] J. Herrick, S. Jun, J. Bechhoefer, and A. Bensimon, J. Mol. Biol. **320**, 741 (2002).
[14] B. Kämpfer, Ann. Phys. (Leipzig) **9**, 605 (2000).
[15] A. Okabe, B. Boots, K. Sugihara, and S. N. Chiu, *Spatial Tessellations: Concepts and Applications of Voronoi Diagrams*, 2nd ed. (John Wiley & Sons Ltd, Chichester, 2000).
[16] F. Jarai-Szabo and Z. Neda, Physica A **385**, 518 (2007).
[17] M. Tomellini and M. Fanfoni, Phys. Lett. A **380**, 2031 (2016).
[18] J. D. Axe and Y. Yamada, Rhys. Rev. B **34**, 1599 (1986).
[19] K. Sekimoto, Physica A **135**, 328 (1986).
[20] P. Mulheran and J. H. Harding, Acta Metall. Mater. **39**, 2251 (1991).
[21] D. Crespo and T. Pradell, Phys. Rev. B **54**, 3101 (1996).
[22] S. Jun, H. Zhang, and J. Bechhoefer, Phys. Rev. E **71**, 011908 (2005).
[23] J. Farjas and P. Roura, Phys. Rev. B **78**, 144101 (2008).
[24] E. Ben-Naim and P. L. Krapivsky, Phys. Rev. E **54**, 3562 (1996).